THE EFFECTS OF MICROSTRUCTURE ON CAVITY NUCLEATION AND PROPAGATION FOR UHTCS USED IN HCV

J. Liang, C. Wang
Center for Composite Materials, Harbin Institute of Technology, Harbin 150080, China

Abstract: In the modern war, the speed of communication searching and release becomes faster and faster, many countries put their eyes on the Hypersonic Cruiser Vehicle (HCV) which can fill current capability shortfalls in exiting weapons. The high-temperature behavior of ultrahigh temperature ceramics (UHTCs) As the thermal protecting material become more and more important. But The microstructure in a polycrystalline ceramic material is complex, such as, the distribution of the grain size, grain-boundary ledges and cavities. The inhomogeneity may give rise to nonuniform local stress distribution. A model has been developed for cavity nucleation and propagation in UHTCs containing viscous grain boundary phase. The critical stress for cavity nucleation and the local stress concentration factor are first calculated. Then the propagation and connectivity time for one and two cavities on a gain size boundary are calculated respectively. The reason of cavity nucleation on gain-boundary ledges has been explained, the influence for propagation time on local stress has been discussed and the propagation time for cavities at different site of a gain size boundary has been compared.

Keywords: HCV ; UHTCs ; cavity nucleation ; cavity propagation ; grain boundary

1. INTRODUCTION

In the modern war, the speed of communication searching and release becomes faster and faster, many countries put their eyes on the Hypersonic Cruiser Vehicle (HCV) which can fill current capability shortfalls in exiting weapons. The attractive strengths, inoxidizability and non-ablation, exhibited by many ceramics at elevated temperatures, have led to a great interest in developing them as thermal protect materials. The mechanical property at elevated temperature for a long time has been decayed as grain boundaries namely ,GB, are coated with a film of glassy second-phase material[1] deriving from processing requirement. Commonly, the process of creep on ceramics is that cavities are presumed to nucleate and grow within the field of influence of a local stress concentrator and coalesce to form a microcrack, the latter then grows to a critical size and failure [2]. Cavity nucleation has generally been considered as a thermally activated process that occurs through the clustering or condensation of individual vacancies, theoretical analyses indicate that stresses considerably in excess of the applied stress are required to form a spherical cavity. The prime reasons for stress concentration are the distribution of different grain size and GB ledges or particles. High densities of GB ledges have been observed [3, 4] in aluminas with continuous viscous phase suggests that ledges may have been the preferred site for the nucleation of two-grain facet cavities. The life time of creep ceramics is controled by the cavity expansion and coalescent time which is decided by the sliding of the grain.

In the present paper, a model has been developed for cavity nucleation and propagation in UHTCs containing viscous grain boundary phase. Critical stress involving the effects of various shapes of cavities has been calculated using classical Becker-Doring nucleation theory. The stress concentration factor considering the height and density of GB ledges has been derived. The effection of grain sliding on cavity propagation has been discussed. The analytic expression of propagation time on a single cavity has been derived. The interaction for two cavities has been analyzed. The rate of propagation speed for two cavities has been compared. The results indicate that the main influence factor for cavity propagation is local stress. The reason of cavity nucleation at GB ledges with continuous viscous phase has been discussed.

2. CAVITY NUCLEATION

Cavity nucleation has generally been considered as a thermally activated process that occurs through the clustering or condensation of individual vacancies, theoretical analyses indicate that stresses considerably in excess of the applied stress are required to form a spherical cavity.

2.1. Critical stress on cavity nucleation

The critical stress on cavity nucleation, P*, is calculated using classical nucleation theory. The specific formulas can be seen in Ref. [5]. The material properties used in the calculation are taken from Ref. [6]. The different angles formed at the GB have been considered. For α=60˚ and α=90˚, the result is summarized in Fig. 1.

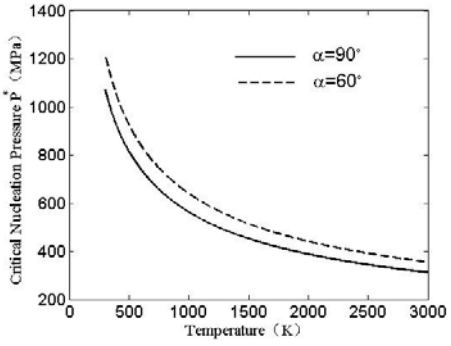

Fig.1 Critical stress for cavity nucleation on different shapes.

Fig. 1 indicates that whatever the cavity shape is, the critical stress for cavity nucleation at 2000K is about 400MP, however, the experimentation shows that the far

field applied stress at 1500˚C for the same material is nearly 45MP which is 8-9 times lower than the calculative value. The discrepancy between the predicted critical stress and the experimental far field applied stress values implies that the existence of a micro-structurally will induce stress concentration.

2.2. The Model of GB Ledges and Stress Concentration

The simplified model for ledges at GB containing continuous viscous phase is shown in Fig. 2. (a)

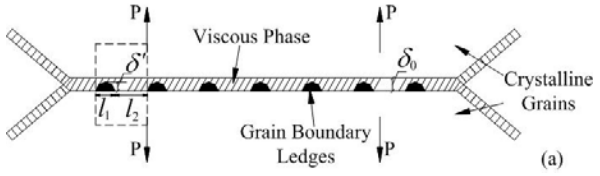

Fig. 2. (a) The ledges at GB contained continuous viscous phase.

, where δ_0 is the uniform thickness of GB viscous phase, δ' is the height of the GB ledges, l_1 is the width of the ledges and l_2 is the distance between them. The distances between GB ledges in the model are assumed as being equal when the distance shown in experiments is between 100 to 200nm [1]. The height is also assumed equally.

The local strain rate at GB without ledges for ceramics containing continuous viscous phase is given by Ref. [7].

$$(1)\quad \dot{\varepsilon}_1 = \frac{3\sigma_1}{8\eta}\left(\frac{2\delta_0}{\sqrt{3}L}\right)^3 \frac{3(1-\xi_1)^3(1+2\xi_1)^3}{(1+2\xi_1)^3+2(1-\xi_1)^3}$$

σ_1 and ε_1 are the local stress and strain at GB without ledges, respectively, and L is the length of a grain size. Analogously, the local strain rate at GB containing ledges is given by

$$(2)\quad \dot{\varepsilon}_2 = \frac{3\sigma_2}{8\eta}\left(\frac{2\delta_{eq}}{\sqrt{3}L}\right)^3 \frac{3(1-\xi_2)^3(1+2\xi_2)^3}{(1+2\xi_2)^3+2(1-\xi_2)^3}$$

where δ_{eq} is the equivalent thickness of GB viscous phase. The model of δ_{eq} is given by Fig. 2. (b)

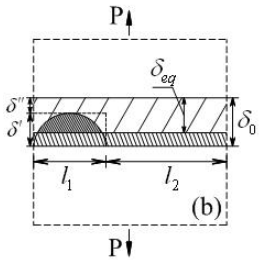

Fig. 2. (b) The theory model of the equivalent thickness of GB viscous phase δ_{eq}.

When calculating the capacity of GB ledges, the elliptical shape is simplified as rectangular. The thickness of GB viscous phase has been decreased due to GB ledges. The equivalent height of GB ledges and the equivalent thickness of GB viscous phase are respectively given by

$$(3)\quad \delta'_{eq} = \frac{\delta' l_1}{l_1+l_2} \text{ and } \delta_{eq} = \delta_0 - \delta'_{eq} = \frac{\delta'' l_1 + \delta_0 l_2}{l_1+l_2}$$

Assume that the deformation is uniform, it requires that

$$(4)\quad \dot{\varepsilon} = \dot{\varepsilon}_1 = \dot{\varepsilon}_2 \text{ and } \varepsilon = \varepsilon_1 = \varepsilon_2$$

The stresses, σ_1 and σ_2, are related to the external stress σ^∞ in the equilibrium equation

$$(5)\quad \sigma^\infty = \sigma_1 V_1 + \sigma_2 V_2$$

Incorporating equations (1)-(5), the local stress at GB contained ledges can be expressed as

$$(6)\quad \frac{\sigma_2}{\sigma_\infty} = \left\{V_2 + n^3\left[\frac{(1-\xi_2)^3(1+2\xi_2)^3}{(1-n\xi_2)^3(1+2n\xi_2)^3}\bullet\frac{(1+2n\xi_2)^3+2(1-n\xi_2)^3}{(1+2\xi_2)^3+2(1-\xi_2)^3}\right](1-V_2)\right\}^{-1}$$

where

$$(7)\quad n = \frac{\delta_{eq}}{\delta_0} = \frac{\alpha\beta+1}{\beta+1}, \alpha = \frac{\delta''}{\delta_0} \text{ and } \beta = \frac{l_1}{l_2}$$

α is defined as the coefficient for the degree of roughness of GB, which characterizes the height of GB ledges and β as the density coefficient of GB ledges.

The local stress is transferred into the hydrostatic pressure on the viscous phase, which can be seen in Ref. [8]. The hydrostatic pressure at the triple grain junction, P_T, and P_M at the midpoint of the two grain channel, are respectively obtained as

(8)

$$-\frac{P_T}{\sigma^\infty} = \frac{3/2}{\left(1+2\left(\frac{1-\xi_2}{1+2\xi_2}\right)^3\right)}\left\{V_2 + n^3\left(\frac{(1-\xi_2)^3(1+2\xi_2)^3}{(1-n\xi_2)^3(1+2n\xi_2)^3}\right)\left(\frac{(1+2n\xi_2)^3+2(1-n\xi_2)^3}{(1+2\xi_2)^3+2(1-\xi_2)^3}\right)(1-V_2)\right\}^{-1}$$

and

(9)

$$-\frac{P_M}{\sigma^\infty} = \left(\frac{9}{4} - \frac{3/4}{\left(1+2\left(\frac{1-\xi_2}{1+2\xi_2}\right)^3\right)}\right)\left\{V_2 + n^3\left(\frac{(1-\xi_2)^3(1+2\xi_2)^3}{(1-n\xi_2)^3(1+2n\xi_2)^3}\right)\left(\frac{(1+2n\xi_2)^3+2(1-n\xi_2)^3}{(1+2\xi_2)^3+2(1-\xi_2)^3}\right)(1-V_2)\right\}^{-1}$$

2.3. Discussion

In Fig. 3, $-P_T/\sigma^\infty$ and $-P_M/\sigma^\infty$ are illustrated by equation (10) and (11), with the influence of α, β and V_2, respectively.

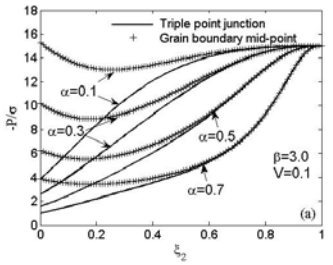

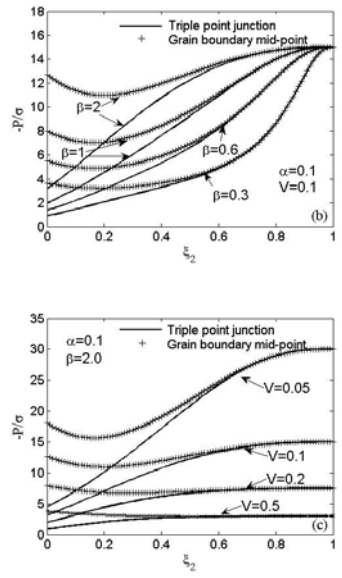

Fig.3. The local stress concentration factor (a) The influence of α for stress concentration. (b) The influence of β for stress concentration. (c) The influence of V_2 for stress concentration.

Fig. 3 shows that, for specific V_2, α and β, the hydrostatic tension in the viscous phase at the two-grain channels and the triple-point junctions for grains containing GB ledges may reach 10 or even 25 times that of the external stress σ^{∞}, which approximately explains the cavity nucleation stress calculated is much higher than the far field applied stress observed in experiments. Fig. 3 also shows that when the creep initiates (ξ_2=0), the hydrostatic tension at the midpoint of a two-grain boundary channel is always four times greater than that at the triple point junction. Fig. 3. (a) indicates that, the hydrostatic tension increase with the increment of the ledge heights. In Fig. 3. (b), it can be seen that, the hydrostatic tension grows proportionally with the GB ledges density. From Fig. 3. (c), the increasing of hydrostatic tension is determined by the increase of the non-homogeneous level of distribution on GB ledges.

3. CAVITY PROPAGATION

3.1. Single Cavity Propagetion

For single cavity Evans [9] has already give the complete propagation model due to the sliding of the grain, Fig.4 shows the propagation process.

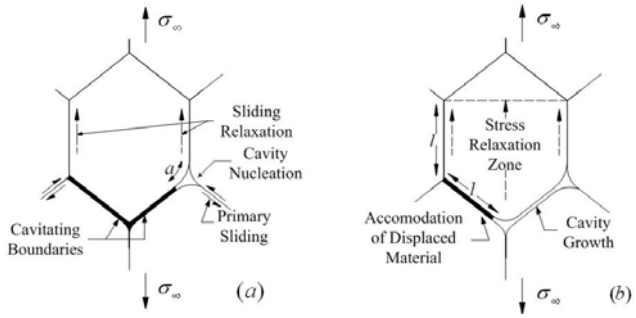

Fig.4. The propagation model for single cavity at three grain junction. (a) before the propagation. (b) after the propagation.

The rate of propagation speed is given by

$$\dot{a} = \frac{32\delta_0^2}{3\eta(2-a/l)^4 l}\left[\sigma_\infty - \frac{3(2-a/l)^2\gamma_l}{8\delta_0}\right] \quad (10)$$

Suppose σ_∞ as $\frac{2\gamma_l}{\delta_0}$ $\frac{3\gamma_l}{\delta_0}$ $\frac{4\gamma_l}{\delta_0}$ $\frac{10\gamma_l}{\delta_0}$ $\frac{20\gamma_l}{\delta_0}$, respectively, the result shows in Fig.5.

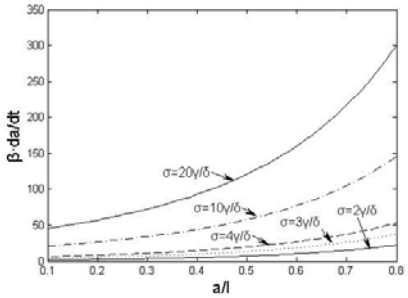

Fig.5. The influence of external stress on the rate of propagation speed

Fig.5 shows that the rates of propagation speed increase with the increase of external stress. For failure time, a great part of it focuses on the very beginning of the propagation process.

The analytic expression of propagation time on a single cavity can be derived form integral (10) from 0 to 1

$$t_p = \frac{\eta l^2}{4\delta_0\gamma_l}\left(\frac{1}{2}m^{\frac{3}{2}}\ln\frac{(\sqrt{m}+2)(\sqrt{m}-1)}{(\sqrt{m}+1)(\sqrt{m}-2)} - m - \frac{7}{3}\right) \quad (11)$$

where $m = \frac{8\delta_0\sigma_\infty}{3\gamma_l}$

The relationship between propagation time and external stress can be obtained as Fig.6.

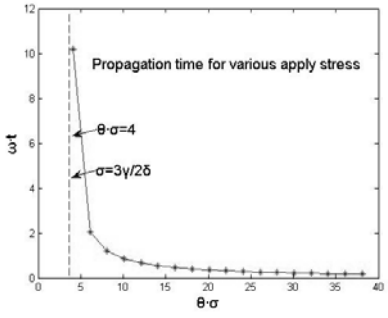

Fig.6. The relationship between propagation time and external stress

In Fig.6, it can be seen that the propagation time increase with the decrease of the external stress. There is a critical

value of the external stress which is $\sigma_c > \frac{3\gamma_l}{2\delta_0}$. ω and θ are all relate to only material constant, where, $\omega = \frac{4\delta_0\gamma_l}{\eta l^2}$ and $\theta = \frac{8\delta_0}{3\gamma_l}$. Under normal exteral stress the approximate propagation time is

(12) $t_p \approx (0.25 \sim 0.45)\frac{\eta}{\sigma_\infty}\left(\frac{l}{\delta_0}\right)^2$

3.2. The Coalescent and Propagation of Two Cavities

For several cavities, the interrelationship can not be ignored. By way of simplify, we concern only tow cavities, one is at the three grain junction the other is at the two grain channel. The simplify model is shown in Fig.7.

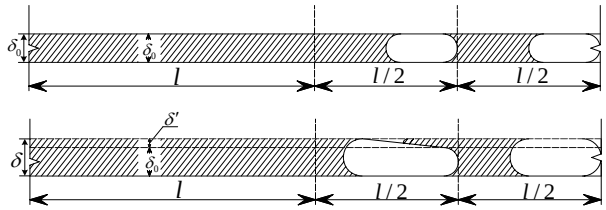

Fig.7. The simplify model for two cavities at three grain junction and two grain channel respectively

Three assumption have been made for calculate the propagation time. (1) The direction of cavity propagation is uniform; (2) the rate of propagation speed of the second cavity is not effect by viscous phase flow through the first cavity and grain boundary; (3) stress relaxation is ignored. For the first cavity we can obtain the same result as above

(13) $\sigma(x) = \frac{1}{\delta}\left[2\gamma_l + \frac{3\eta\dot{\delta}x}{2\delta^2}(3l - 2a - x)\right] \quad (0 < x < \frac{3}{2}l)$

Derivate (13) by x at x=0 (at the end of viscous phase) is

(14) $\left.\frac{d\sigma}{dx}\right|_{x=0} = \frac{3\eta\dot{\delta}}{2\delta^3}(3l - 2a)$

The average flow speed of viscous phase is [10]

(15) $v_l = -\frac{\delta^2}{3\eta}\left(\frac{d\sigma}{dx}\right)$

Submit (14) into (15) is

(16) $v_l = -\frac{\delta^2}{3\eta}\frac{3\eta\dot{\delta}}{2\delta^3}(3l - 2a) = -\frac{\dot{\delta}}{\delta}(\frac{3}{2}l - 2a)$

Submit δ and $\dot{\delta}$ into (16) we can see

(17) $v_l = -\dot{a}$

Employ the same method for the second cavity, and notice that the thickness of viscous phase δ and the velocity of grain sliding $\dot{\delta}$ are the same for both first and second cavities, we can obtain that

(18) $\dot{b} = \left(\frac{1/2 - b/l}{3/2 - a/l}\right)\dot{a}$

Submit (10) into (18) we can obtain

(19) $\dot{b} = \left(\frac{1/2 - b/l}{3/2 - a/l}\right)\left(\frac{9\delta_0^2\sigma_\infty}{2\eta l\left(\frac{3}{2} - a/l\right)^4} - \frac{3\gamma_l\delta_0}{\eta l\left(\frac{3}{2} - a/l\right)^2}\right)$

Then we can compare the rate of propagation speed using equation (19), the result shows in Fig.8.

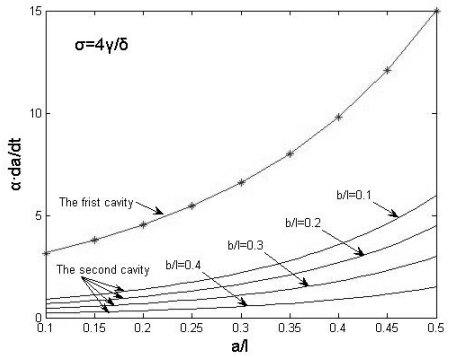

Fig.8. The comparison of the rate of propagation speed for the tow cavities.

Fig.8 indicates that the rate of propagation speed for the first cavity is much higher than the second, as the influence of the nearby grain channel. We can find that the rate of propagation speed for the second cavity decrease with the increase of the size of the cavity, when b/l proximity to 1/2 the rate proximity to zero. The reason for this impossible case is the assumption (2) is too strong. So consider the contribution of the viscous phase flow through the first cavity and grain boundary, use calculus of differences and modify the b by b' (the contribution of the viscous phase), $b' = \frac{(\delta_n - \delta_{n-1})\bullet a_n}{\delta_n}$. Then the propagation length for first and second cavitis at the same time can be obtain as Fig.9. In the Fig.9 for the same style curve, the above one is stand for the first cavity and the lower side one is sand for the second cavity.

In this condition (get $\alpha = 1$), $x = 0.3l$ is the critical position that the cavities propagate and coalesce finish at the same time. When $x > 0.3l$ propagation time for the first cavity is short than the coalescent time, and for $x < 0.3l$ propagation time is long. Then we can first

determine the domination time, and we can calculate the propagation time accurately by the above method.

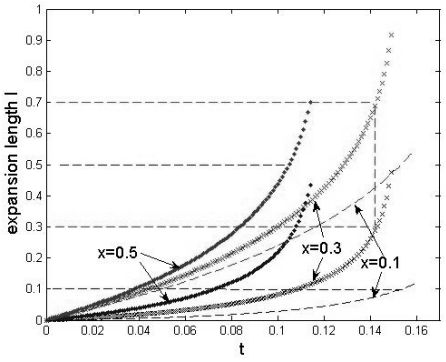

Fig.9. The critical position for the two cavities propagation and coalescent at the same time

4. CONCLUSION

The present work addresses the problem why cavities nucleate easily at GB ledges and give the explanation on the interrelationship between cavites during their propagation process. The local stress concentration can increase the hydrostatic tension in the viscous phase at the two-grain channels and the triple point junctions 10 times or more. The principle for the change of hydrostatic tension with the height of the ledges, the GB ledges density and the non-homogeneous level of distribution on GB ledges has been demonstrated. It can be seen that the stress concentration factor increases when the size of grain-boundary ledges, the density or the non-homogeneous level is high. For a single cavity the rates of propagation speed increase with the increase of external stress. The analytic expression of propagation time on a single cavity can be derived and the propagation time increase with the decrease of the external stress. For several cavities, the associate between them is the displacement and the velocity of grain sliding. The rate of propagation speed for the first cavity is much higher than the second, as the influence of the nearby grain channel. For calculate the propagation time with several cavities, the most important step is to estimate the dominant process, the propagation time and the coalescent time which is shorter. Then the real propagation time can be calculated. Moreover, it should be mentioned that the development of cavity nucleation can cause much energy loss; the analysis above is only applicable at the initiation of the cavity nucleation. Study on stress field coupled with energy dissipation remains an attractive problem, which needs further attention.

REFERENCES

[1] K.S. Chan and R.A. Page: J. Am. Ceram. Soc. Vol.76 (1993), P. 803.
[2] R. Raj: Advances in Fracture Research. Vol.4 (1989), P. 2769.
[3] R.A. Page, J. Lankford and K.S. Chan: J. Am. Ceram. Soc. Vol.70 (1987), P.137.
[4] J. Lankford, K.S. Chan and R.A. Page: Fracture Mechanics of Ceramics. Vol.7 (1986), P.327.
[5] J.E. Marion, A.G. Evans, M.D. Drory and D.R. Clarke: Acta Metall. Vol.31 (1983), P.1445.
[6] M.D. Thouless and A.G. Evans: J. Am. Ceram. Soc. Vol. 67 (1984), P.721.
[7] J.R. Dryden, D. Kucerovsky, D.S. Wilkinson, et al: Acta Metall. Vol. 37 (1989), P.2007.
[8] N. Dey, K.J. Hsia and D.F. Socie: Acta Metall. Vol. 45 (1997), P.4117.
[9] A.G.Evans, A.Rana: Acta Metall. Vol.28(1980), P.129.
[10] R.J. Fields, M.F. Ashby: Phil. Mag. Vol.33(1976), P.33.